Geometric Processing of Digital Images of the Planets

Kathleen Edwards
U. S. Geological Survey, Branch of Astrogeology, 2255 North Gemini Drive, Flagstaff, AZ 86001

ABSTRACT: New procedures and software have been developed for geometric transformation of images to support digital cartography of the planets. The procedures involve the correction of spacecraft camera orientation of each image with the use of ground control and the transformation of each image to a Sinusoidal Equal-Area map projection with an algorithm which allows the number of transformation calculations to vary as the distortion varies within the image. When the distortion is low in an area of an image, few transformation computations are required, and most pixels can be interpolated. When distortion is extreme, the location of each pixel is computed. Mosaics are made of these images and stored as digital databases. Completed Sinusoidal databases may be used for digital analysis and registration with other spatial data. They may also be reproduced as published image maps by digitally transforming them to appropriate map projections.

INTRODUCTION

GLOBAL IMAGE MAPS of the planets are being compiled by the U.S. Geological Survey from digital images returned by planetary spacecraft (Batson, 1987). These global maps, termed Digital Image Models or DIMs, consist of single images and mosaics of images in a map-projected raster format. The DIMs are processed in four levels: (1) radiometric correction, (2) correction for geometric distortion and transformation to a map projection, (3) photometric compensation, and (4) controlled mosaicking. This paper describes the second level — geometric processing — which consists of (1) correcting the camera orientation, (2) removing the electronic distortions introduced by the imaging system, and (3) transforming the point-perspective geometry of the original image to a map projection. The map projections used are described in detail by Snyder (1982).

Historically, a variety of cartographic projections were used for geometric transformation and mosaicking. For areas near the equator, Mercator was used; in the middle latitudes, Lambert Conformal; and near the poles, Polar Stereographic. Very high resolution images were sometimes transformed to a Transverse Mercator, and very low resolution images were often transformed to an Orthographic or some other global projection. Individually projected images were then used to make mosaics. Problems arose because many images overlapped projection boundaries, therefore requiring transformation to two or even three map projections, and because the transformation algorithm could not accommodate extreme scale discrepancies between original images (such as global views that included the limb, or horizon) and map projections.

In the new procedure, all images are transformed to a single map projection, the Sinusoidal Equal-Area, which can be used over an entire planet without being segmented into zones. All mosaics are made and stored in this projection and are transformed to desired map projections as needed. A new algorithm has been developed to transform images that have extreme scale variations.

GEOMETRIC TRANSFORMATIONS

The algorithm used for geometric transformations finds a point on the original image for every point on the projected image. It is important to remember, however, that a pixel on the original image is unlikely to retain either its size or shape on the projected image. The method used here allows a single pixel to be projected to several pixels as required to portray the original pixel on the projected image. Most transformations require the solution of complex mapping equations to describe how the image should be projected. Solving the full mapping equations to project every pixel of an image is not practical because it is too time consuming on most minicomputers. The rigorous computation is, therefore, made for only a small percentage of points in the image. Intermediate points are projected by bilinear interpolation, a much faster and simpler algorithm.

Bilinear interpolation consists of defining a rectangular grid overlay for the projected (or output) image and using mapping equations to determine the location of each corner of each grid cell on the original image. The coordinates of the corners of each rectangular grid cell are then used to find the coefficients for the transformation (bilinear interpolation) of the cell in the projected image to a general quadrilateral in the original image: i.e.,

$$X' = AXY + BX + CY + D \quad (1)$$
$$Y' = EXY + FX + GY + H \quad (2)$$

where X' is the original line, Y' is the original sample, X is the projected line, Y is the projected sample, and A through H are the coefficients.

Once the coefficients have been computed, the locations of points inside the cell are then computed by this simple transformation. A uniform grid overlay was used with the old method, whereas the new algorithm allows subdivision of grid cells where required to model the output projection accurately. An iterative series of tests is used to determine the optimum subdivision of each rectangle. First, the four corners of the rectangular cell are calculated from the full mapping equations. The center of the rectangle is then calculated both by bilinear interpolation and by using the mapping equations. If the bilinear interpolation differs from the mapping equations by more than 0.5 pixels, the rectangle is divided into quarters. The process is repeated until the bilinear interpolation error is less than 0.5 pixels or until the location of each pixel in the rectangle has been calculated.

Figures 1 and 2 illustrate the transformation of an image of the Uranian satellite Miranda from spacecraft perspective (Figures 1a and 1b) to Sinusoidal Equal-Area projection (Figures 1c and 1d) and from Sinusoidal to Polar Stereographic (Figures 2a, 2b, 2c, and 2d). Along with the image maps, graphics showing the gridding are provided. The largest cells in the Sinusoidal grid of Figure 1d are empty; no part of the Voyager image is projected to those areas. The south polar part of the Sinusoidal is densely gridded because image shapes in that area are so different from the shapes of the same area in the center left of the Voyager image of Figure 1b. The grid becomes less densely gridded away from the pole, until the limb is reached. The stair steps at the bottom of the image are caused by allowing projection computations to include longitudes beyond the ±180° limits of the Sinusoidal array. A larger grid spacing can be used if this boundary is not treated as a discontinuity; the redundant data will be ignored when stored Sinusoidal images are changed to other map projections.

PHOTOGRAMMETRIC ENGINEERING AND REMOTE SENSING,
Vol. 53, No. 9, September 1987, pp. 1219–1222

0099-1112/87/5309–1219$02.25/0

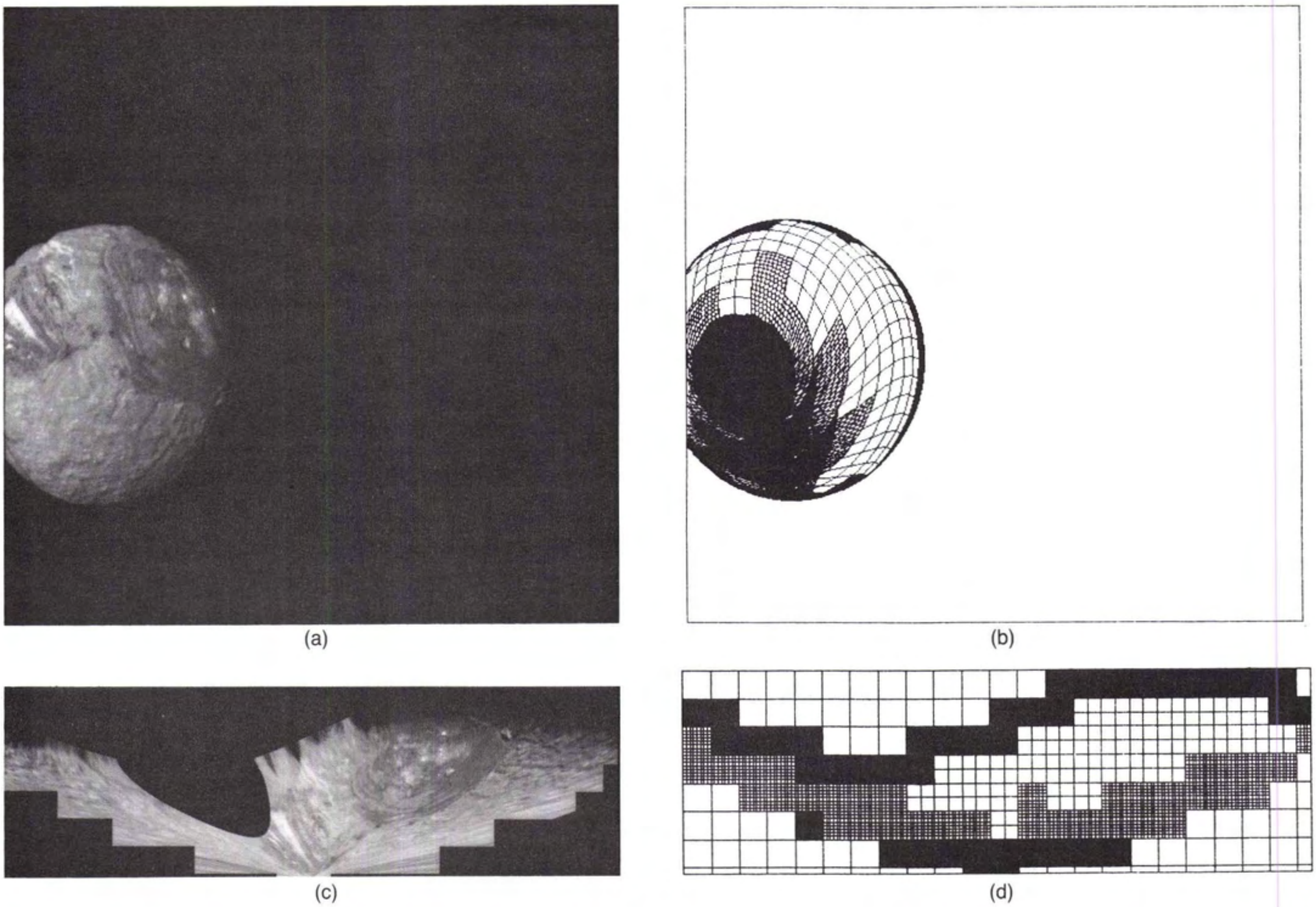

FIG. 1. The transformation of a spacecraft image to the Sinsoidal Equal Area database format. (a) A Voyager image (Picno. 1477U2-001) of Miranda. (b) The gridding scheme used to transform the image to the Sinusoidal. (c) Sinusoidal Equal-Area projection of the Voyager image. (d) The grid in Figure 1b as it would appear in the Sinusoidal projection.

When a part of the Sinusoidal database of Figure 1a is transformed to a standard map projection of Figure 2d, the Sinusoidal becomes the input projection (Figures 1c and 2a), and the map projection becomes the output projection. The dense gridding in the bottom center of the output Polar Stereographic grid (Figure 2d) covers the 180° boundary meridian and corresponds to the dense strip on the right and left edges of Figure 2b. No simple interpolation scheme can be used across the boundary meridian of the Sinusoidal database. The transformation is calculated point by point in these areas, and no bilinear interpolation is done.

Meridians and parallels are defined by the edges, rather than the centers, of pixels in order to avoid confusion when arrays are compressed or enlarged. By our convention, the latitude/longitude of a pixel refers to its northwest corner.

CORRECTING CAMERA DISTORTIONS

The vidicon cameras used by the Viking and Voyager spacecraft have electronic distortions very similar in pattern to the optical distortion in a film camera. These electronic distortions are introduced because the scanning pattern of the electron beam used to read out the charge-stored image vidicon is more "barrel-shaped" than rectangular. Interactions between the charge on the photo-cathode that represents the image itself and the electron beam produce additional complex high-order distortions.

The positions of reseau marks etched on the vidicon image tube are measured before the spacecraft leaves Earth. The distorted positions of the reseau marks on the returned images are identified and compared to the undistorted reseau positions. A 16- by 16-pixel grid spacing is defined for the undistorted image. At each grid intersection a least-squares fit to a pair of general second-order equations is used to calculate the distorted position of that grid intersection: i.e.

$$X = AX{**}2 + BXY + CY{**}2 + DX + EY + F \qquad (3)$$
$$Y' = GX{**}2 + HXY + IY{**}2 + JX + KY + L \qquad (4)$$

where X' is the distorted line position of a reseau mark, Y' is the distorted sample position, X is the undistorted line position, and Y is the undistorted sample position.

This calculation uses only the reseau marks within the region of that intersection (usually within a radius of 120 pixels). The fit is weighted by the distance of each reseau mark from the grid intersection being calculated so that the closest reseau marks have the most influence on the fit. After the distorted positions of all the grid intersections have been calculated, coefficients for bilinear interpolation of the undistorted to the distorted positions in the interior of each grid rectangle are calculated and saved for later use. This method is sufficient to correct 90 percent of the distortions within 0.5 pixels. A small area in each corner has a higher order of distortion than can be removed by these equations; reseau-mark spacing in that area is inadequate to properly describe the distortion.

MAP PROJECTION TRANSFORMATION

All planetary images are transformed to a single map projection (the Sinusoidal Equal-Area) during geometric processing and are mosaicked in that projection to create geometric databases. The map scale is chosen in increments of a power of 2 (1/4 degrees/pixel, 1/8 degrees/pixel, etc.). Any image can there-

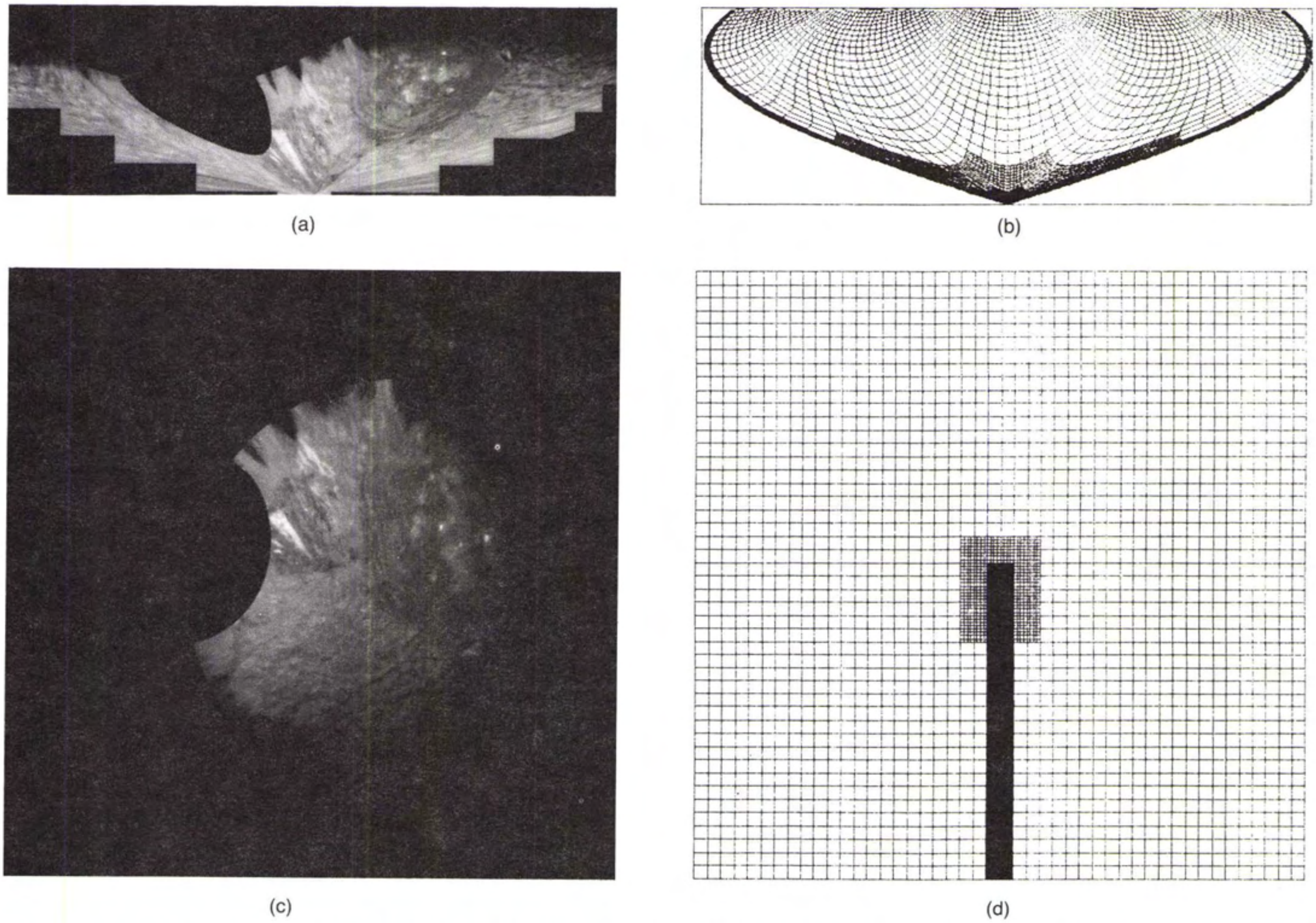

FIG. 2. The transformation from the Sinusoidal Equal Area database to a standard map projection. (a) The Voyager image in Sinusoidal database format. (b) The gridding scheme used to transform from the Sinusoidal format to a Polar Stereographic map projection. (c) Polar Stereographic projection of the Sinusoidal image. (d) The grid in Figure 2b as it would appear in the Polar projection.

fore be mosaicked with any other of another scale by doubling or halving the number of lines and samples in the image as needed, without resampling the image array.

Several parameters are needed to describe the geometry of spacecraft images so that they can be transformed to map projections. They are planet orientation matrix, spacecraft vector, camera orientation matrix (**C**-matrix), focal length of the camera, and radius (or radii, for non-spherical objects) of the planet. The planet orientation matrix is the transformation matrix from the planet coordination system to the Earth Mean Equatorial B1950 or J2000 system (Davies *et al.*, 1983). The spacecraft vector is the position of the spacecraft relative to the center of the planet in B1950 or J2000 and the **C**-matrix is the orientation of the camera relative to B1950 or J2000. The planet orientation matrix is used to rotate the spacecraft vector and the **C**-matrix into the planet coordinate system. Figure 3 is a diagram of the spacecraft vector and camera orientation relative to the planet after the rotation.

The steps required to transform an image are as follows:

(1) Find the map scale and latitude and longitude range covered by the output image in order to determine the required size of the map projection (for example, the map scale of Figure 1c is 1/4 degree/pixel, the latitude range is -90 to $+17$ degrees, the longitude range is -180 to $+180$ degrees, and the size of the projection is 429 by 1114 pixels).

(2) Partition the map projection (Figures 1d or 2c) into a rectangular grid.

(3) For each corner of each partition
   (a) Find the latitude and longitude of the northwest pixel corner of a given line and sample on the map projection;
   (b) Project that latitude and longitude from the planet to the image plane to find the corresponding line and sample on an undistorted image;
   (c) Find the distorted position for that line and sample using the coefficients that were saved during the camera-distortion correction stage.

(4) Test the grid density. Will bilinear interpolation between the grid points be within 0.5 pixels of the calculations when the spacecraft geometry is used? If not, subdivide the grid cell and repeat step (3).

CORRECTING THE CAMERA ORIENTATION MATRIX (C-MATRIX)

The planet orientation and the spacecraft vector are smoothly changing parameters and are reasonably well known, but many factors, such as small unknown errors in yaw, pitch, or roll of the spacecraft, and small errors in knowledge of scan-platform slewing can cause errors in the **C**-matrix predicted on the basis of photogrammetric triangulation (Davies and Katayama, 1983; Wu and Schafer, 1984) or by spacecraft telemetry and ephimerides. These errors are usually less than 0.5 degrees and can be corrected with the use of ground-control points that have been identified in the image. To make the corrections, the ground-control points are identified as measured lines and samples in the image and corresponding latitudes and longitudes on the planet. The latitudes and longitudes and the predicted **C**-matrix are used to find predicted lines and samples. The predicted lines and samples are then compared to the measured lines and samples to determine the angular pointing errors (dX, dY, dZ) in the C-matrix, where dX is proportional to an error in the line direction, dY to an error in the sample direction, and dZ is any

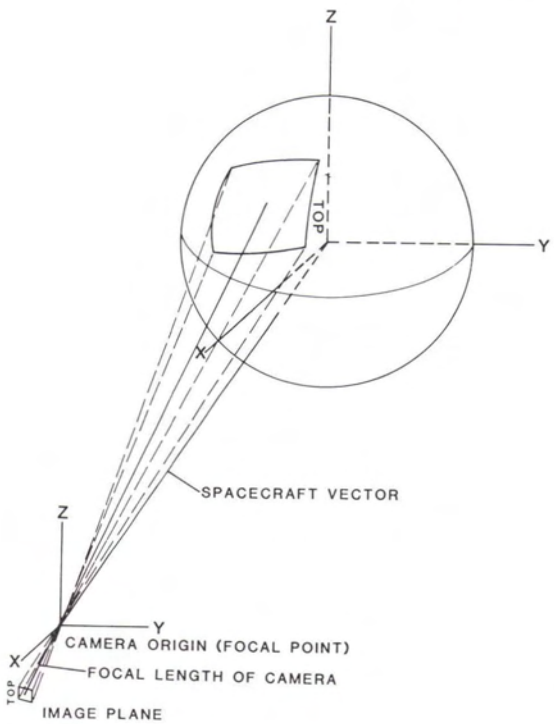

FIG. 3. The spacecraft vector and camera orientation in the planet coordinate system.

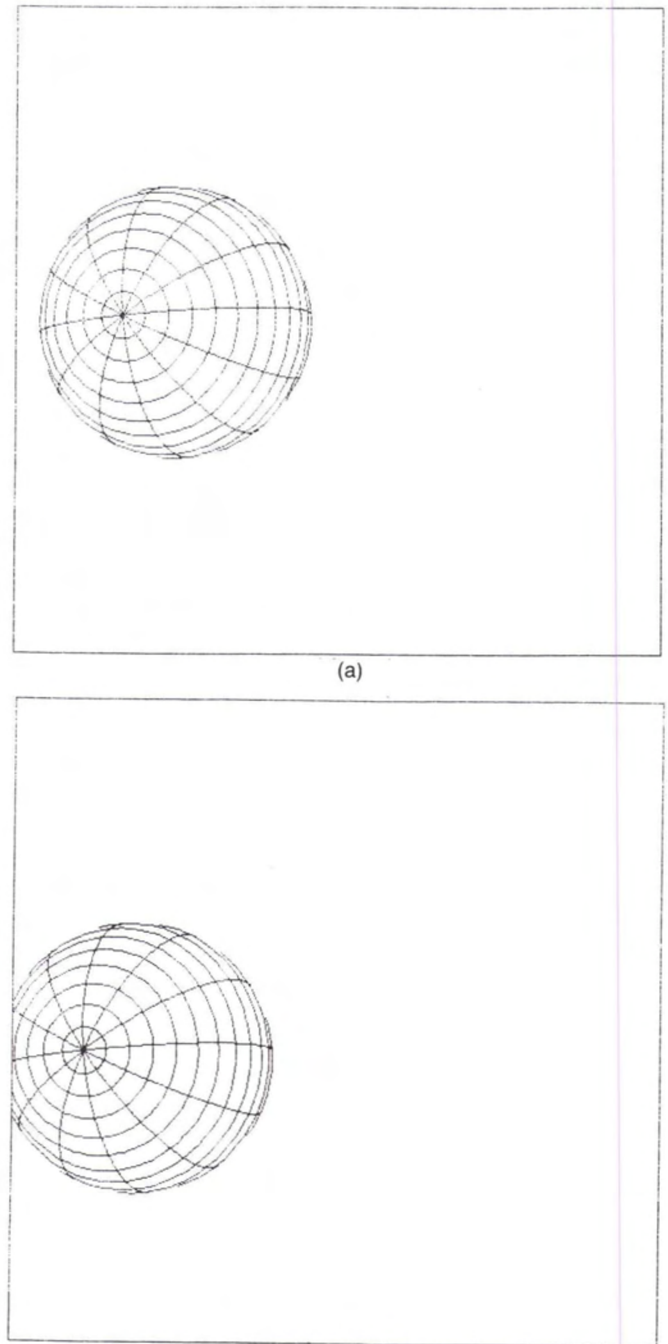

(a)

(b)

FIG. 4. Diagram of the image of Miranda (Figure 1a). (a) Image location prior to correction of the camera orientation matrix (C-matrix). (b) Image location after the C-matrix has been corrected.

rotation needed to correct the pointing. The predicted C-matrix is multiplied by the small changes in pointing to create a new C-matrix in the planet coordinate system. Then the new C-matrix is rotated back to the original coordinate system for permanent storage. Figure 4a is a schematic of the Voyager image in Figure 1. A single control point was used to correct the predicted C-matrix, shifting the image frame so that the image of Miranda moved down and to the left (Figure 4b).

CONCLUSIONS

The advantages in the procedures used here over previous techniques are as follows:

- Most algorithms for geometric transformations allow only a single grid spacing over the projected image. This method allows very dense spacing in areas where it is needed and sparse spacing over the rest of the image. Discontinuities can be handled easily, resulting in a cleaner and more accurate final product; no artifacts are created at the poles, at the 180° meridian, or at the limb of the planet.
- Neglecting the effects of topography, the degree to which a spacecraft image can be made to correspond to a map projection depends on the accuracy of the C-matrix used to make the transformation. The more the camera pointing angle deviates from nadir, the more significant C-matrix errors become. The correction method described here has been used successfully to make mosaics of images with large off-nadir viewing angles.
- The use of the Sinusoidal Equal-Area projection as the array upon which all mosaics are compiled and digitally stored has simplified both the compilation and the use of digital maps of the planets.

ACKNOWLEDGMENTS

This work was supported by the Planetary Geology and Geophysics Program, Planetary Division, Office of Space Science, National Aeronautics and Space Administration, under contract W-15, 814, and by the Jet Propulsion Laboratory, Mars Observer Project.

REFERENCES

Batson, R. M., 1987. Digital cartography of the planets: New methods, its status, and its future. *Photogrammetric Engineering and Remote Sensing,* v. 53, no. 9, pp. 1211–1218.

Davies, M. E., V. K. Abalakin, J. H. Lieske, P. M. Seidelmann, A. T. Sinclair, A. M. Sinzi, B. A. Smith, and Y. S. Tjuflin, 1983. Report of the IAU working group on cartographic coordinates and rotational elements of the planets and satellites: 1982. *Celestial Mechanics,* v. 29, pp. 309-321.

Davies, M. E., and F. Y. Katayama, 1983. The 1982 control net of Mars. *Journal of Geophysical Research,* v. 88, no. B-9, pp. 7503-7504.

Snyder, J. P., 1982. *Map Projections Used by the U.S. Geological Survey.* Geological Survey Bulletin 1532, U.S. Government Printing Office, 313 p.

Wu, S. S. C., and F. J. Schafer, 1984. Mars control network: *Proceedings of the 50th Annual Meeting,* American Society of Photogrammetry, 2, pp. 456-463.

(Received 27 April 1987; accepted 22 May 1987)